Scientific Research Publishing

International Journal of Geosciences, 2023, 14, 603-618
https://www.scirp.org/journal/ijg
ISSN Online: 2156-8367
ISSN Print: 2156-8359

Technique for Estimating the Cone Bearing Smoothing Parameters

Erick Baziw

Baziw Consulting Engineers Ltd., Vancouver, Canada
Email: ebaziw@bcengineers.com

How to cite this paper: Baziw, E. (2023) Technique for Estimating the Cone Bearing Smoothing Parameters. *International Journal of Geosciences*, **14**, 603-618.
https://doi.org/10.4236/ijg.2023.147032

Received: June 12, 2023
Accepted: July 22, 2023
Published: July 25, 2023

Abstract

Cone penetration testing (CPT) is an extensively utilized and cost effective tool for geotechnical site characterization. CPT consists of pushing at a constant rate an electronic cone into penetrable soils and recording the resistance to the cone tip (q_c value). The measured q_c values (after correction for the pore water pressure) are utilized to estimate soil type and associated soil properties based predominantly on empirical correlations. The most common cone tips have associated areas of 10 cm^2 and 15 cm^2. Investigators also utilized significantly larger cone tips (33 cm^2 and 40 cm^2) so that gravelly soils can be penetrated. Small cone tips (2 cm^2 and 5 cm^2) are utilized for shallow soil investigations. The cone tip resistance measured at a particular depth is affected by the values above and below the depth of interest which results in a smoothing or blurring of the true bearing values. Extensive work has been carried out in mathematically modelling the smoothing function which results in the blurred cone bearing measurements. This paper outlines a technique which facilitates estimating the dominant parameters of the cone smoothing function from processing real cone bearing data sets. This cone calibration technique is referred to as the so-called *CPSPE* algorithm. The mathematical details of the *CPSPE* algorithm are outlined in this paper along with the results from a challenging test bed simulation.

Keywords

Cone Penetration Testing (CPT), Geotechnical Site Characterization, Optimal Estimation, Iterative Forward Modelling (IFM), Monte Carlo Techniques, Calibration

1. Introduction

The Cone Penetration Test (CPT) is an extensively published geotechnical *in-situ* tool which is utilized to identify and characterize sub-surface soil [1] [2] [3] [4]

[5]. In CPT a steel cone is pushed vertically into the ground at a typical standard rate of 2 cm per second and data are recorded at constant rate during penetration (typically every 2 cm). The cone penetrometer has electronic sensors to measure penetration resistance at the tip (q_c) and friction in the shaft (f_s) during penetration. A CPT probe equipped with a pore-water pressure sensor is called a piezo-cone (CPTU cones). For piezo-cones with the filter element right behind the cone tip (the so-called u_2 position) it is standard practice to correct the recorded tip resistance and sleeve friction for the measured pore pressure. **Figure 1** [6] outlines the equations for obtaining sleeve friction and tip resistance where corrections are made for measured pore water pressures and differences in area (e.g., tip net area ratio and end area sleeve).

Figure 2 [7] illustrates the dimensions of the two most commonly utilized penetrometers which have cone tips with associated areas of 10 cm^2 and 15 cm^2. Larger cone tip penetrometers (33 cm^2 and 40 cm^2) are utilized to penetrate gravelly soils. Small cone tips (2 cm^2 and 5 cm^2) are utilized for shallow soil investigations. **Figure 3** illustrates the comparable size of cone tips with areas of 2 cm^2, 5 cm^2, 10 cm^2, 15 cm^2 and 40 cm^2.

The distortions which effect the cone tip measurements are two-fold: 1) the cone tip resistance is smoothed/blurred [9] [10] [11] [12] where cone tip values measured at a particular depth are affected by values above and below the depth of interest, and 2) the cone bearing measurements are susceptible to anomalous peaks and troughs due to the relatively small diameter cone tip penetrating sandy, silty and gravelly soils [1] [13]. The "high" peaks result from the penetration of interbedded gravels and stones and the "low" peaks results from the penetration of softer materials or local pore pressure build-up. This additive measurement noise can be significantly challenging to remove or minimize. The cones with relatively smaller cone tips are significantly more susceptible to the anomalous peaks and troughs while the cones with larger cone tips are more susceptible to the smoothing of the cone tip measurements. This suggests that cones with relatively larger cone tips would be more desirable if accurate deblurring techniques could be implemented (*i.e.*, minimize additive noise and penetrate soils with high resistance).

The blurring effect of cone bearing measurements has been extensively studied. Boulanger and DeJong [9] summarize the numerous studies carried out where elastic analyses, nonlinear analyses (cavity expansion and axisymmetric models), and physical measurements (centrifuge models, 1 g physical models, and field data) were utilized. Based upon this work a mathematical model was developed to describe the distortions of the cone penetrometer measurements as the cone penetrates variable weak and strong layers. This mathematical model was outlined by Boulanger and DeJong [9]. In general terms, a cone weighting function is applied to the true cone bearing measurements where true cone bearing measurements are averaged over approximately 60 cone diameters at the cone tip. The Cone Bearing Weighting Function (*CBWF*) described by Boulanger and DeJong [9] is a function of several parameters and baseline values are

utilized for these when implementing the *CBWF* for estimating true cone bearing values from blurred measurements. The research purpose and focus of the work outlined in this paper was to develop a technique to estimate the *CBWF* parameters based upon real CPT data sets. The technique (so-called *CPSPE* algorithm) which estimates the *CBWF* parameters is subsequently outlined along with a challenging test bed simulation.

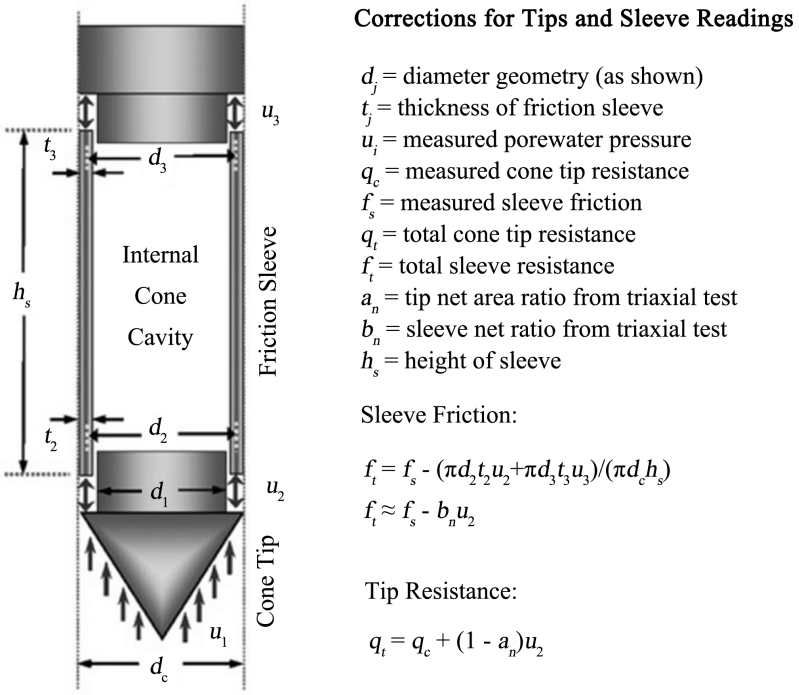

Figure 1. Determination of total cone resistance and total sleeve friction [6].

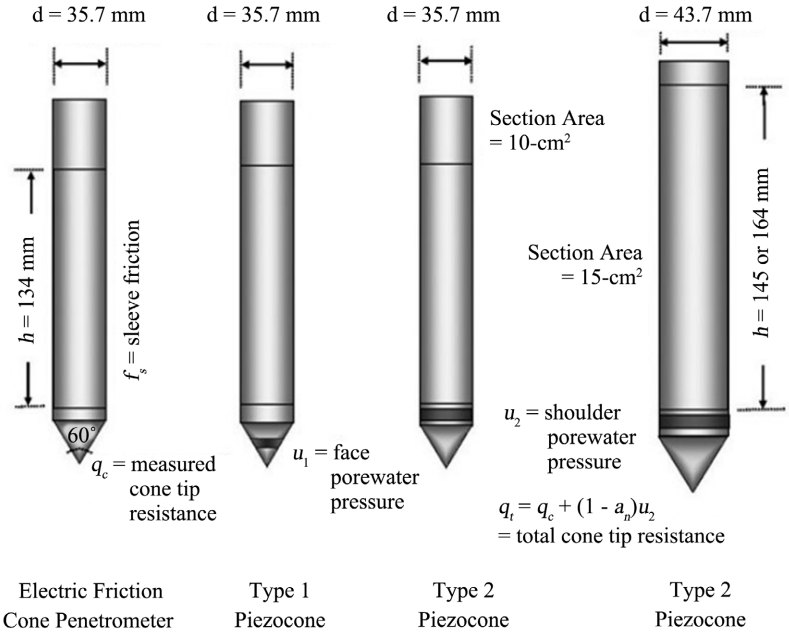

Figure 2. Standard 10 cm² and 15 cm² penetrometers [7].

Figure 3. 5 cm^2, 10 cm^2, 15 cm^2 and 40 cm^2 penetrometers [8].

2. Mathematical Background

2.1. CPT Cone Bearing Model

The cone tip resistance measured at a particular depth is affected by the values above and below the depth of interest as illustrated in **Figure 4** [9]. The results in an averaging or blurring of the true values (q_v) values [9] [10] [11] [12].

The measured cone penetration tip resistance q_c can then be described as

$$\begin{aligned} q_c(z) &= \sum_{j=1}^{N\times\left(\frac{d_c}{\Delta}\right)} w_c(j)\times q_v\left(\Delta_{qc}+j\right)+v(z) \\ \Delta_{qc} &= \left(z-\Delta_{wc}\right), \Delta_{wc} = N\times\left(\frac{d_c}{2\Delta}\right), N=60 \end{aligned} \tag{1}$$

where

z the cone depth;

d_c the cone tip diameter;

Δ the q_c sampling rate;

$q_c(z)$ the measured cone penetration tip resistance;

$q_v(z)$ the true cone penetration tip resistance;

$w_c(z)$ the $q_v(z)$ averaging function;

$v(z)$ additive noise.

In Equation (1) it assumed that w_c averages q_v over 60 cone diameters centered at the cone tip. Boulanger and DeJong [9] outline how to calculate w_c below.

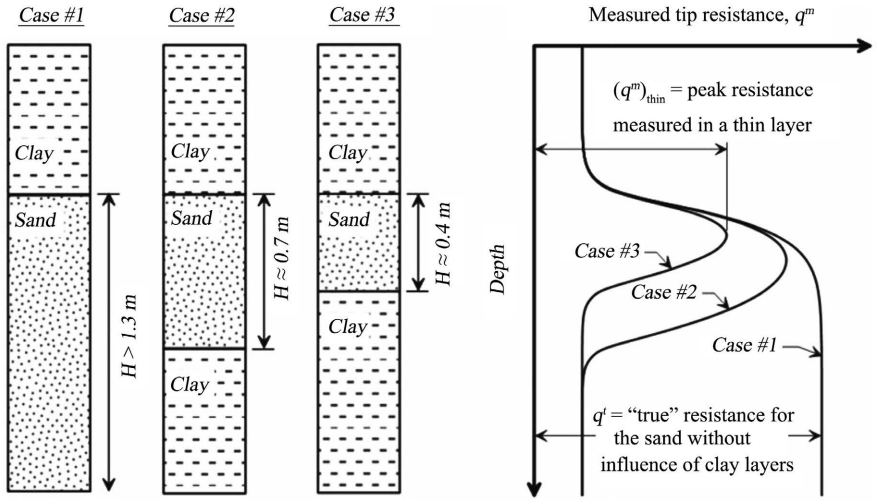

Figure 4. Schematic of thin layer effect for a sand layer embedded in a clay layer [9].

$$w_c = \frac{w_1 w_2}{\sum w_1 w_2} \tag{2a}$$

$$w_1 = \frac{C_1}{1+\left|\left(\frac{z'}{z'_{50}}\right)^{m_z}\right|} \tag{2b}$$

$$z' = \frac{z - z_{tip}}{d_c} \tag{2c}$$

$$C_1 = \begin{cases} 1 \text{ for } z' \geq 0 \\ 1+\dfrac{z'}{8} \text{ for } -4 \leq z' < 0 \\ 0.5 \text{ for } z' < -4 \end{cases} \tag{2c}$$

$$z'_{50} = 1 + 2\left(C_2 z'_{50,ref} - 1\right)\left[1 - \frac{1}{1+\left(\frac{q_{v,z'=0}}{q_{v,z'}}\right)^{m_{50}}}\right] \tag{2d}$$

$$C_2 = \begin{cases} 1 \text{ for } z' > 0 \\ 0.8 \text{ for } z' \leq 0 \end{cases} \tag{2e}$$

$$w_2 = \sqrt{\frac{2}{1+\left(\frac{q_{v,z'}}{q_{v,z'=0}}\right)^{m_q}}} \tag{2c}$$

where

w_1 accounts for the relative influence of any soil decreasing with increasing distance from the cone tip.

w_2 adjusts the relative influence that soils away from the cone tip will have on

the penetration resistance based on whether those soils are stronger or weaker.

z' the depth relative to the cone tip normalized by the cone diameter.

The four main parameters which influence w_c are $z'_{50,ref}$, m_z, m_{50}, and m_q. Boulanger and DeJong [9] outline the baseline values for these parameters as $z'_{50,ref} = 4.0$, $m_z = 3.0$, $m_{50} = 0.5$, and $m_q = 2$. Boulanger and DeJong also set $N = 60$ in Equation (1) (*i.e.*, $-30 \le z' \le 30$). The value of $N = 60$ cone diameters was implemented due to w_c being close to zero for distance exceeding 30 cone diameters from the cone tip based upon the previously specified baseline cone smoothing parameters. The *CBWF* w_c for varying $q_{v,z'}/q_{v,z'=0}$ ratios is illustrated in **Figure 5**.

The cone penetration unnormalized averaging function w'_c (Equation (2a)) for varying $q_{v,z'}/q_{v,z'=0}$ ratios is illustrated in **Figure 6**. The interaction between varying soil layers can result in highly variable cone bearing averaging functions. For example, **Figure 7** illustrates the w_c function for the case where above the cone tip $q_{v,z'}/q_{v,z'=0} = 10$, from the cone tip to an extra depth of 0.16 m $q_{v,z'}/q_{v,z'=0} = 10$, from the cone tip plus 0.16 m to an extra depth of 0.24 m $q_{v,z'}/q_{v,z'=0} = 0.1$, and at greater depths $q_{v,z'}/q_{v,z'=0} = 1.0$.

The effect on w'_c of varying the four cone averaging parameters is illustrated in **Figures 8-10**. **Figure 8(a)** and **Figure 8(b)** illustrate that increasing the value of $z'_{50,ref}$ increases the breadth of w'_c. **Figure 9(a)** and **Figure 9(b)** illustrate the effect of increasing and decreasing the value of m_z on the shape of w'_c. **Figure 10(a)** illustrates that decreasing the value of m_q results in a greater influence on w'_c for higher $q_{v,z'}/q_{v,z'=0}$ ratios. **Figure 10(b)** illustrates the effect on the shape of w'_c for $m_{50} = 0.8$.

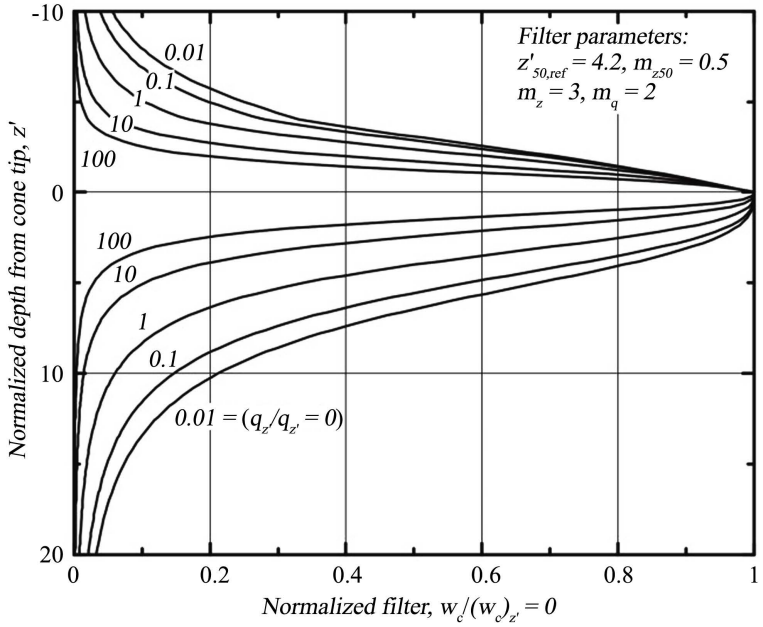

Figure 5. Normalized cone penetration filter versus normalized depth from the cone tip ($q_{t,z'}/q_{t,z'=0} = 0.01, 0.10, 10, 100$) [9].

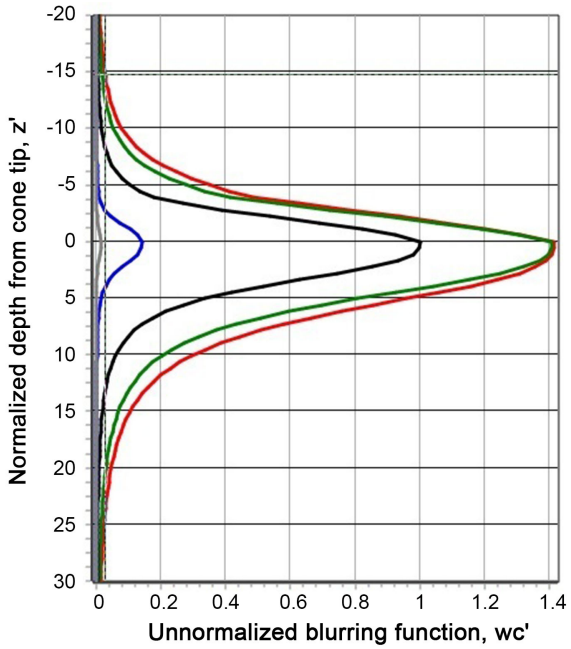

Figure 6. Unnormalized cone penetration filter, w_c', versus normalized depth from the cone tip with lines for $q_{v,z'}/q_{v,z'=0}$ = 0.01 (red), 0.1 (green), 1 (black), 10 (blue) and 100 (grey).

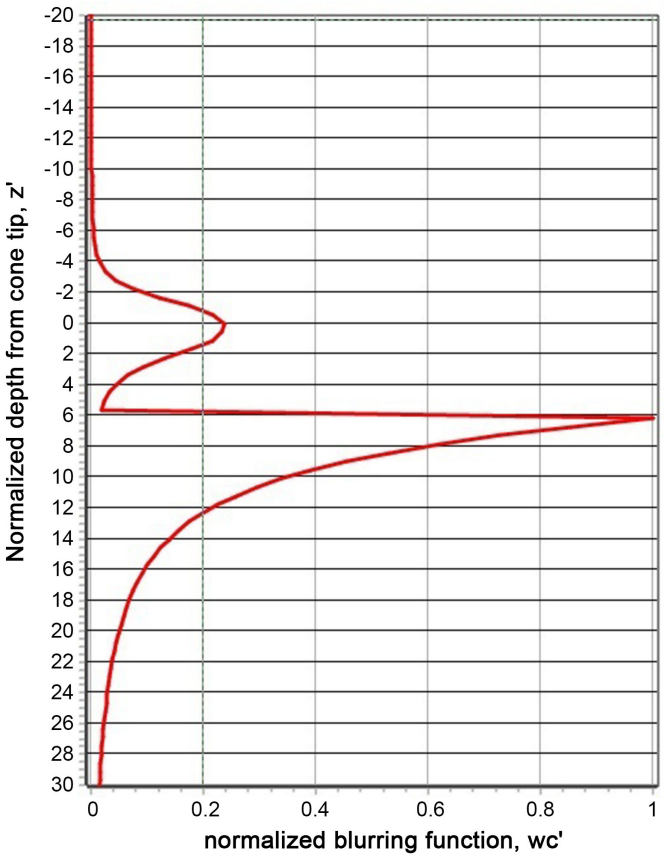

Figure 7. Normalized blurring function w_c.

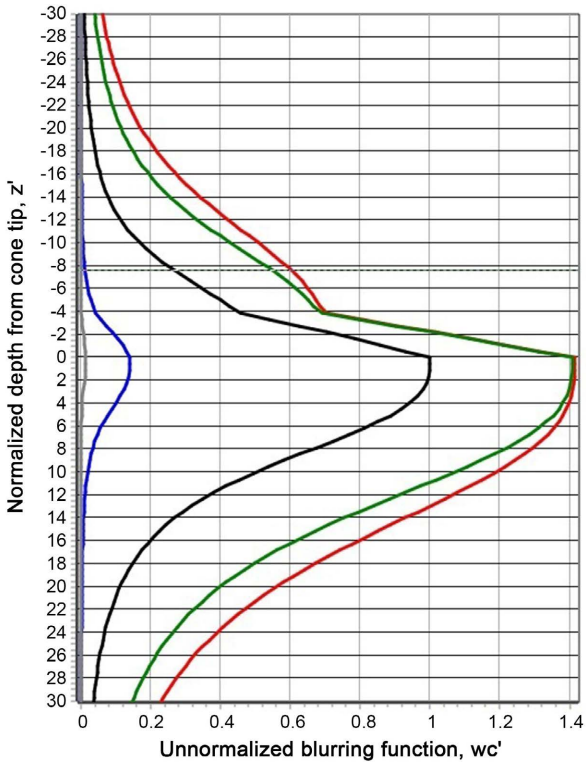

(a)

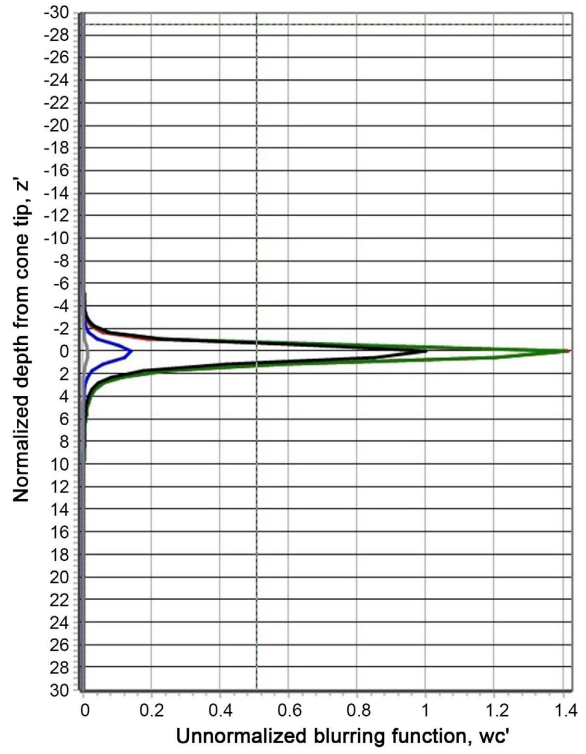

(b)

Figure 8. Unnormalized cone penetration filter, w_c', versus normalized depth from the cone tip with lines for $q_{v,z'}/q_{v,z'=0}$ = 0.01 (red), 0.1 (green), 1 (black), 10 (blue) and 100 (grey). (a) $z'_{50,ref}$ =10 and (b) $z'_{50,ref}$ =1.

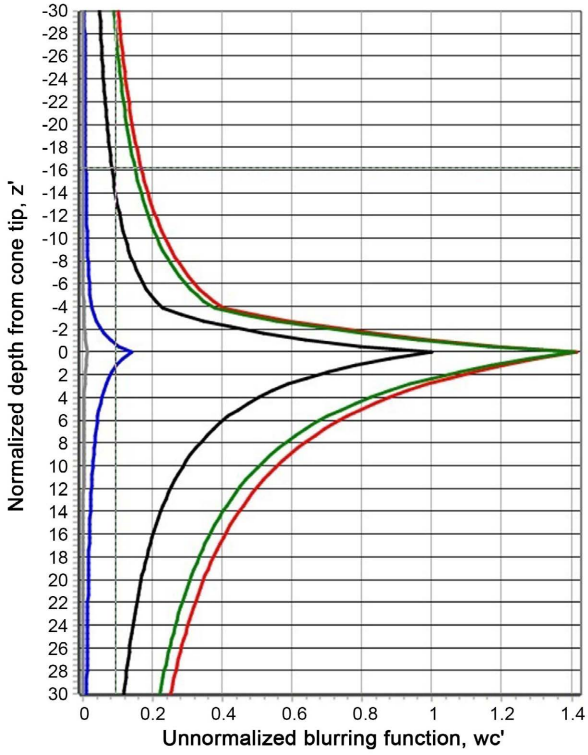

(a)

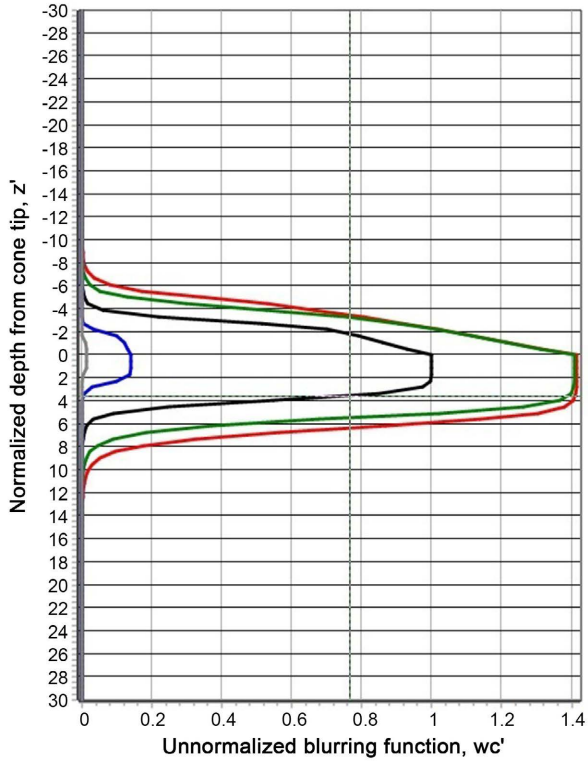

(b)

Figure 9. Unnormalized cone penetration filter, w_c', versus normalized depth from the cone tip with lines for $q_{v,z'}/q_{v,z'=0}$ = 0.01 (red), 0.1 (green), 1 (black), 10 (blue) and 100 (grey). (a) m_z = 10 and (b) m_z = 1.

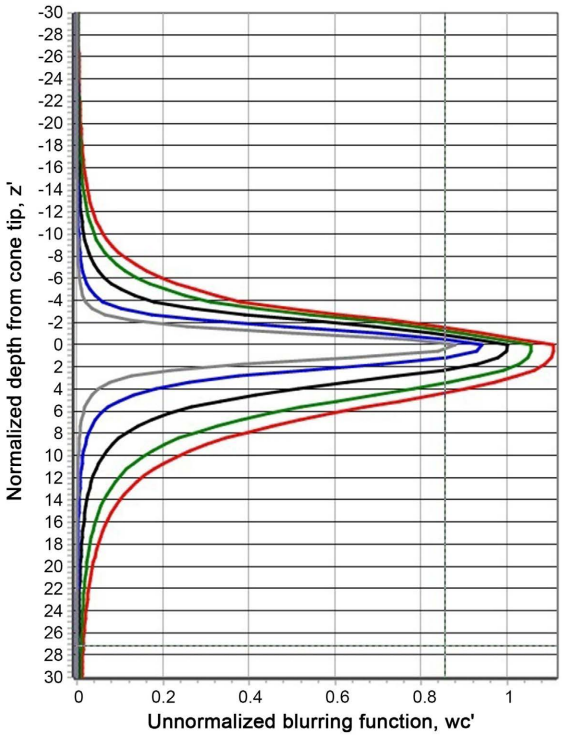

(a)

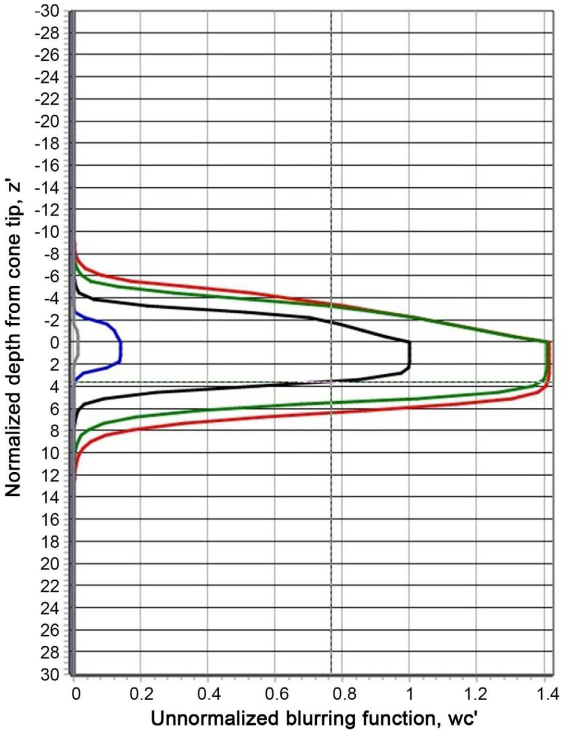

(b)

Figure 10. Unnormalized cone penetration filter, w_c', versus normalized depth from the cone tip with lines for $q_{v,z'}/q_{v,z'=0}$ = 0.01 (red), 0.1 (green), 1 (black), 10 (blue) and 100 (grey). (a) m_q = 1 and (b) m_{50} = 0.8.

2.2. Iterative Forward Modeling

Iterative forward modeling (IFM) is a parameter estimation technique which is based upon iteratively adjusting the parameters until a user specified cost function is minimized. The desired parameter estimates are defined as those which minimize the user specified cost function. The IFM technique which is utilized within the *CPSPE* algorithm for estimating the *CBWF* parameters is the downhill simplex method (DSM) originally developed by Nelder and Mead [14]. A simplex defines the most elementary geometric figure of a given dimension: a line in one dimension, the triangle in two dimensions, the tetrahedron in three, etc; therefore, in an N-dimensional space, the simplex is a geometric figure that consists of $N+1$ fully interconnected vertices. The DSM starts at $N+1$ vertices that form the initial simplex. The initial simplex vertices are chosen so that the simplex occupies a good portion of the solution space. In addition, it is also required that a scalar cost function be specified at each vertex of the simplex. The general idea of the minimization is to keep the minimum within the simplex during the optimization, at the same time decreasing the volume of the simplex. The DSM searches for the minimum of the costs function by taking a series of steps, each time moving a point in the simplex away from where the cost function is largest. The simplex moves in space by variously reflecting, expanding, contracting, or shrinking. The simplex size is continuously changed and mostly diminished, so that finally it is small enough to contain the minimum with the desired accuracy.

3. CPSPE Algorithm

The *CBWF* parameters optimal filter estimation technique is referred to as the *CPSPE* algorithm. The *CPSPE* algorithm relies upon processing known or what is termed in this paper as "well-behaved" cone bearing profiles. This does not necessarily require that the complete cone profile is processed, just portions of the q_c profile which are known or "well-behaved". As more cone bearing data sets are processed the estimates of the *CBWF* parameters become more refined and accurate.

A real data cone bearing profile is considered known if the soil profile has been thoroughly investigated which may include supporting soil logging samples. A "well-behaved" cone bearing profile is defined as containing significantly large depth intervals with constant q_c values (greater than the transition depth uncertainties). **Figure 11** illustrates a schematic of two cone bearing profiles where it is assumed that they are "well-behaved" (profile 1) and known (profiles 2) real data cone bearing measurements (e.g., q_{c21}) and associated soil transition interface (e.g., z_{21}) for each profile. Areas where uncertainties for the location of the interface depth are identified by light grey transparent boxes (*i.e.*, z_{11}, z_{12} and z_{13}). It is not expected that the depth interval of the uncertainty transition would exceed 60 to 80 cone diameters. This is equivalent to 2.14 m to 2.85 m for a 10 cm^2 cone and 4.28 m to 5.71 m for a 40 cm^2 cone. The reasons for this assump-

tion are two-fold. 1) The work of Boulanger and DeJong [9] where they set $N = 60$ in Equation (1) due to w_c being close to zero for distance exceeding 30 cone diameters from the cone tip utilizing the baseline *CBWF* parameters. 2) The simulation of variable values of the *CBWF* parameters as illustrated in **Figures 8-10**.

In the *CPSPE* algorithm a simplex is initialized based upon the unknown *CBWF* parameters ($z'_{50,ref}$, m_z, m_{50}, and m_q) and unknown transition depths (e.g., z_{11}, z_{12} and z_{13}). For example, for the two profiles illustrated in **Figure 11** there are seven unknowns $z'_{50,ref}$, m_z, m_{50}, m_q, z_{11}, z_{12} and z_{13}. This implies that the DSM starts at 8 vertices that form the initial simplex. A scalar cost function is determined at each vertex of the simplex by utilizing Equations (1) and (2). The initial simplex vertices are chosen so that the simplex occupies a good portion of the solution space (e.g., minimum and maximum values of unknown parameters). Alternatively, several iterations (e.g., within a while loop) of the DSM could be implemented where for each iteration initial samples are drawn for the unknown parameters utilizing a Monte Carlo technique [15]. The iteration which results in the smallest overall error residual would be the best estimate of the unknown parameters.

The *CPSPE* algorithm incorporates the following steps:

1) Specify unknowns and initial vertices of the simplex. For the case illustrated in **Figure 11** we have seven unknowns (8 vertices): *CBWF* parameters ($z'_{50,ref}$, m_z, m_{50}, and m_q) and unknown transition depths (e.g., z_{11}, z_{12} and z_{13}). If the initial simplex index is denoted as k, we have initial unknowns $zk'_{50,ref}$, mk_z, mk_{50}, mk_q, zk_{11}, zk_{12} and zk_{13} ($k = 1$ to 8) for the case illustrated in **Figure 11**.

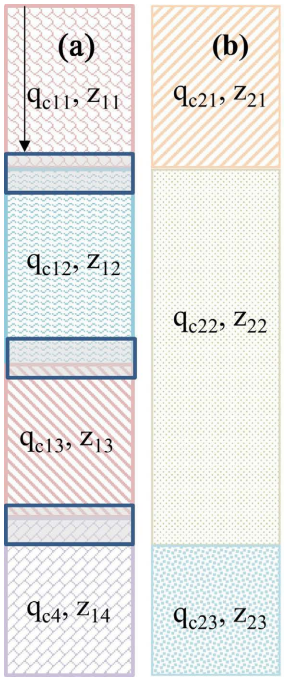

Figure 11. Example of (a) "well-behaved" and (b) known cone bearing profiles.

2) Calculate the Scalar Cost Function (SCF) for each vertex of the initial vertices. The SCF is defined as the Root Mean Square (RMS) difference between the simulated cone bearing values and the measured values for each cone profile under analysis. When initializing the simplex, it is recommend that minimum and maximum values are utilized and/or drawing initial estimates of the unknown parameters from a Monte Carlo technique.

The scalar cost functions are obtained by implementing Equations (1) and (2) for each cone profile under analysis. For the case illustrated in Figure 11 there are two cone profiles ($L = 2$) under analysis. For each vertex and cone profile the true cone bearing value $qk_v(z)$ is a function of the known cone bearing values and the unknown transition depths. For the case of the "well-behaved" cone profile $qk_v\,(z,\ q_{ij},\ zk_{ij})$ (e.g, $q1k_v\,(z,\ q_{ij},\ zk_{ij})$ in Figure 11. For the case of the known cone profile $qk_v\,(z,\ q_{ij})$ (e.g, $q2k_v\,(z,\ q_{ij})$ in Figure 11. The equations for the simulated cone bearing measurements (qlk_c), cone bear smoothing function (wk_c) and *SCFk* are outlined below.

$$\begin{aligned} qlk_c(z) &= \sum_{j=1}^{N\times\left(\frac{d_c}{\Delta}\right)} wk_c(j)\times qlk_v\left(\Delta_{qc}+j\right) \\ \Delta_{qc} &= \left(z-\Delta_{wc}\right),\ \ \Delta_{wc} = N\times\left(\frac{d_c}{2\Delta}\right) \end{aligned} \tag{3a}$$

where l denotes the cone profile under analysis.

N is set to the largest assumed value (*i.e.*, $N = 40$) where w_c goes to zero as previously outlined.

wk_c is obtained from Equation (2) for $zk'_{50,ref}$, mk_z, mk_{50}, mk_q

$$\begin{aligned} SCFk &= \sum_{l=1}^{L}\sum_{z=0}^{D}\left(ql_m(z)-qlk_c(z)\right)^2 \\ SCFk &= \sqrt{SCFk} \end{aligned} \tag{3b}$$

where ql_m is the measured cone bearing for profile l, D is the maximum depth and L is the total number of cone profiles under analysis (*i.e.*, $l = 1$ *to* L).

3) compare the cost function for each vertex and determine the lowest error "best" and highest error "worst" vertices;

4) sequentially locating first the reflected, then if necessary, the expanded, and then if necessary, the contracted vertices, and calculating for each the corresponding cost function and comparing it to the worst vertex; if at any step the cost function of the new trial point is less than the value at the worst vertex; then this vertex is substituted as a vertex in place of the current worst vertex;

5) if the process in step 4 does not yield a lower error value than the previous worst, then the other vertices are shrunken towards the best vertex;

6) at each stage of shrinking, the distances between vertices are calculated and compared to a set tolerance value to check if the simplex has become sufficiently small for termination of the estimation; when the test criterion is reached, the previous best vertex becomes the solution;

7) at each stage of shrinking, the cost function values at the vertices is compared to a set minimum value to check if the error residual has become suffi-

ciently small for termination of the estimation; when the test criterion is reached, the previous best vertex becomes the solution.

CPSPE Test Bed Example

The performance of the *CPSPE* algorithm was evaluated by processing a challenging test bed simulation where a single cone bearing profile having both known and "well-behaved" interfaces is processed. Figure 12 illustrates three cone bearing profiles. The red trace in Figure 12 is the true cone bearing profile q_v which has q_v values of 0.5 MPa (0 m to 3 m), 50 MPa (3 m to 12 m), 20 MPa (12 m to 18 m), 10 MPa (18 m to 23 m), and 40 MPa (23 m to 40 m). The black and blue trace are measured cone bearing profiles where Equations (1) and (2) are implemented with the true red cone bearing trace inputted.

A relatively large 40 cm^2 cone was specified in this simulation (less susceptible to the previously outlined anomalous peaks and troughs but are more susceptible to the smoothing of the cone tip measurements). The blue trace in Figure 12 had the *CBWF* parameters set to the baseline values ($z'_{50,ref} = 4$, $m_z = 3$, $m_{50} = 0.5$, and $m_q = 2$). The black trace in Figure 12 had the *CBWF* parameters set to $z'_{50,ref} = 6$, $m_z = 1.5$, $m_{50} = 1.0$, and $m_q = 3$. The known interfaces are located at 3 m and 23 m. The "well-behaved" interfaces are located at 12 m and 18 m (identified by light grey transparent rectangles).

The *CPSPE* algorithm is applied on the black trace of Figure 12 where it is initially assumed that the baseline values are valid. In this test bed simulation there are 6 unknowns ($z'_{50,ref}$, m_z, m_{50}, m_q, and interfaces at 12 m and 18 m). Table 1

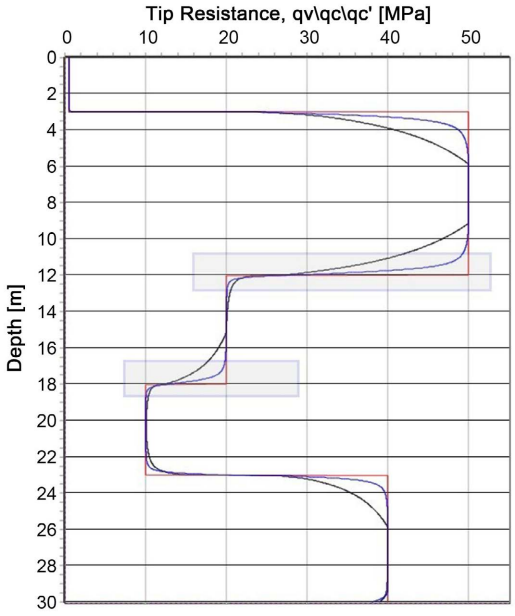

Figure 12. Test bed simulation red trace is the true cone bearing profile, blue trace is the measured cone bearing profile where the *CBWF* parameters are set to the baseline values and black trace is the measured cone bearing profile where the *CBWF* parameters set to $z'_{50,ref} = 6$, $m_z = 1.5$, $m_{50} = 1.0$, and $m_q = 3$.

Table 1. *CPSPE* algorithm settings and optimal estimates.

	$z'_{50,ref}$	m_z	m_{50}	m_q	Unknown Depth1 [m]	Unknown Depth2 [m]
Minimum	2	0.1	0.01	0.1		
Maximum	9	6	3	6		
Interface Transition Range					9 to13	16 to 19
True Values	6.0	1.50	1.0	3.0	12.0	18.0
CPSPE Estimates	6.0	1.50	1.0	3.0	12.0	18.0

outlines the parameters set as input into the *CPSPE* algorithm. In Table 1 the minimum and maximum values of *CBWF* parameters are specified. These limits are applied within the IFM portion of the *CPSPE* algorithm. Table 1 also outlines the uncertainty of the interface transitions (gray areas in Figure 12) for interfaces located at 12 m (9 m to 13 m) and 18 m (16 m to 19 m). In the *CPSPE* algorithm a Monte Carlo technique is utilized where the initial simplex within the IFM portion of the algorithm is initialized with *CBWF* parameters within the minimum and maximum ranges specified in Table 1. The *CPSPE* algorithm is implemented eighty times (eighty simplex initializations). The *CPSPE* estimates are defined as the *CPSPE* algorithm output which results in the lowest SCF (Equation (3b)). Table 1 outlines the *CPSPE* optimal estimates which are identical to the true values.

4. Conclusion

The cone penetrometer test (CPT) consists of pushing at a constant rate an electronic penetrometer into penetrable soils and recording cone bearing (q_c), sleeve friction (f_c) and dynamic pore pressure (u) with depth. The measured q_c, f_s and u values are utilized to estimate soil type and associated soil properties. Cone bearing measurements at a specific depth are blurred or averaged due to q_c values being strongly influenced by soils within 10 to 40 cone diameters from the cone tip. The blurring of the cone tip measurements is mathematically described as the multiplication of a Cone Bearing Weighting Function (*CBWF*) with the true cone bearing values. This paper has outlined an algorithm (so called *CPSPE* algorithm) which obtains optimal estimates of the parameters defining the *CBWF*. The *CPSPE* algorithm is applied on real q_c data sets which are known or "well-behaved". A challenging test bed simulation has demonstrated that the *CPSPE* algorithm can derive accurate estimates of the parameters defining the *CBWF*. This would allow for the calibration of cones of varying sizes based on real q_c data sets.

Conflicts of Interest

The author declares no conflicts of interest regarding the publication of this paper.

References

[1] Lunne, T., Robertson, P.K. and Powell, J.J.M. (1997) Cone Penetrating Testing: In Geotechnical Practice. E & FN Spon, London.

[2] Robertson, P.K., Campanella, R.G., Gillespie, D. and Greig, J. (1986) Use of Piezometer Cone Data. *Proceedings of American Society of Civil Engineers*, *ASCE*, *In-Situ* 86 *Specialty Conference*, Blacksburg, 23-25 June 1986, 1263-1280.

[3] Robertson, P.K. (1990) Soil Classification Using the Cone Penetration Test. *Canadian Geotechnical Journal*, **27**, 151-158. https://doi.org/10.1139/t90-014

[4] ASTM D6067/D6067M-17 (2017) Standard Practice for Using the Electronic Piezocone Penetrometer Tests for Environmental Site Characterization and Estimation of Hydraulic Conductivity. ASTM International, West Conshohocken.

[5] Cai, G.J., Liu, S.Y., Tong, L.Y. and Du, G.Y. (2006) General Factors Affecting Interpretation and Corrections of Primary Data from Piezocone Penetration Test (CPTU). *Journal of Engineering Geology*, **14**, 632-636. (In Chinese)

[6] Ladd, C.C., Germaine, J.T., Lancellotta R. and Jamiolkowski, B. (1985) New Developments in Field and Lab Testing of Soils. *Proceedings of the* 11*th International Conference on Soil Mechanics and Foundation Engineering*, *Vol.* 1, San Francisco, 12-16 August 1985, 57-154.

[7] de Ruiter, J. (1971) Electric Penetrometer for Site Investigations. *Journal of the Soil Mechanics and Foundations Division*, **97**, 457-472. https://doi.org/10.1061/JSFEAQ.0001552

[8] Robertson, P.K. and Cabal, K.L. (2012) Guide to Cone Penetration Testing for Geotechnical Engineering. 5th Edition, Gregg Drilling & Testing, Inc., Signal Hill, 10.

[9] Boulanger, R.W. and DeJong, T.J. (2018) Inverse Filtering Procedure to Correct Cone Penetration Data for Thin-Layer and Transition Effects. In: Hicks, M.A., Pisanò, F. and Peuchen, J., Eds., *Cone Penetration Testing* 2018, CRC Press, London, 25-44.

[10] Baziw, E. and Verbeek, G. (2021) Cone Bearing Estimation Utilizing a Hybrid HMM and IFM Smoother Filter Formulation. *International Journal of Geosciences*, **12**, 1040-1054. https://doi.org/10.4236/ijg.2021.1211055

[11] Baziw, E. and Verbeek, G. (2022) Identification of Thin Soil Layers Utilizing the q_m*HMM-IFM* Algorithm on Cone Bearing Measurements. In: Lemnitzer, A. and Stuedlein, A.W., Eds., *Geo-Congress* 2022, ASCE Press, Reston, 505-514. https://doi.org/10.1061/9780784484036

[12] Baziw, E. and Verbeek, G. (2022) Methodology for Obtaining True Cone Bearing Estimates from Blurred and Noisy Measurements. In: Gottardi, G. and Tonni, L., Eds., *Cone Penetration Testing* 2022, CRC Press, London, 115-120. https://doi.org/10.1201/9781003308829-9

[13] Baziw, E. and Verbeek, G. (2021) Implementation of Kalman Filtering Techniques for Filtering CPT Cone Bearing Measurements. *The DFI* 46*th Annual Conference on Deep Foundations Conference Proceedings*, Las Vegas, 12-15 October 2021, 53-67.

[14] Nelder, J.A. and Mead, R. (1965) A Simplex Method for Function Optimization. *The Computer Journal*, **7**, 308-313. https://doi.org/10.1093/comjnl/7.4.308

[15] Baziw, E. (2011) Incorporation of Iterative Forward Modeling into the Principle Phase Decomposition Algorithm for Accurate Source Wave and Reflection Series Estimation. *IEEE Transactions on Geoscience and Remote Sensing*, **49**, 650-660. https://doi.org/10.1109/TGRS.2010.2058122